Millimeter-scale Magnetic Carrier for On-demand Delivery of Magnetic and Non-magnetic Microparticles Suspensions

Tamerlan Srymbetov*, *Student Member, IEEE* Giordano De Angelis*, Arianna Menciassi, *Fellow, IEEE,* and Veronica Iacovacci†, *Member, IEEE*

***Abstract*—The use of magnetic microparticles (MMPs) has recently proven a great potential for biomedical applications, i.e. for drug delivery or magnetic hyperthermia. However, MMPs are typically delivered passively through systemic injection or exploiting tethered drug delivery systems which require percutaneous medical procedures. Here we propose an untethered magnetic carrier for MMPs suspension delivery. This wireless millirobot is capable of precisely releasing MMPs that after delivery are completely decoupled from the carrier and can be manipulated independently by separate magnetic sources. Experiments were performed in an aqueous environment to validate carrier locomotion and controlled release capabilities. The prototyped carrier (overall 41 mm long and 10 mm in diameter) can be wirelessly moved by an external magnet at a distance larger than 10 cm, and, when fixed magnetically, can be triggered by another external magnet (around 6 mm apart) to release a cargo. Magnetic navigation and release activation well fit model predictions with actuation distance errors below 10% based on experimental performance. The carrier proved able to perform controlled release of non-magnetic and magnetic cargoes and was recorded to release approximately 25% of the loaded MMPs suspension with no premature release.**

I. Introduction

Magnetic microparticles (MMPs) and magnetic microrobots are crucial in non-invasive medical applications including magnetically induced hyperthermia, enhanced magnetic resonance imaging, and, when loaded with drugs, targeted drug delivery [1]. MMPs are fully passive, intrinsically safe, and potentially able to access body regions unreachable by conventional interventional tools by leveraging external magnetic control [2, 3].

MMPs are typically delivered in the body through systemic injection or ingestible carriers and then guided to the target location using external magnetic field sources. However, if the target is distant from the injection site, the targeting efficiency, which is defined as the ratio between the amount of MMPs reaching the target with respect to the injected one, drops accordingly [4, 5]. Essentially, a larger traveling distance means a number of path changes, obstacles, physiological forces to withstand, and the need for proper feedback to effectively reach the target site.

Untethered drug delivery systems have been proposed to increase the therapeutic index, limit biodistribution, and perform targeted delivery of therapeutics [6, 7]. Some of them include on-board active components for locomotion and drug-release actuation [6], whereas many others rely on internal permanent magnets (IPMs) that can be wirelessly activated by external magnetic field sources. On-board IPMs can be exploited either to control the navigation of the untethered device and/or to activate cargo release on-demand [8]. However, combining these tasks is not straightforward and appears even more challenging when the cargo is represented by MMPs suspension due to possible interference between different magnetically triggered effects and the risk of cargo sticking within the carrier structure.

Recently, smart solutions combining magnetic navigation and magnetic cargo release were proposed. Sikorski *et al.* developed a flexible catheter capable of releasing a magnetic soft projectile [9]. Li *et al.* [10] proposed an MRI-compatible catheter able to release controlled MMPs aggregates. The solutions proved the possibility of combining magnetic navigation and magnetic cargo release. However, the proposed carriers consist of catheters and include either powering wires or fluidic tubes needed to activate the release mechanism.

Thus, no untethered solution has been proposed so far to deliver MMPs to a target location. On the other hand, many magnetic bistable mechanisms were proposed for performing biopsy [11, 12] and drug delivery [13, 14], which can be of inspiration for our objective.

Given the potential biomedical applications of MMPs, the drawbacks of systemic administration, and the limitations of catheter-like delivery systems, an untethered millimeter-scale tool might be beneficial for a wide set of tasks, especially for those requiring the release of a precise quantity of MMPs on-site.

In this work, we present a novel carrier design for MMPs suspension delivery. We modeled and experimentally tested the proposed design with respect to both locomotion and controlled release. The main goal is to study and develop a magnetically actuated carrier able to efficiently eject MMPs despite the presence of internal magnets. The remainder of the paper is organized as follows, Section II describes the steps

* These authors contributed equally to the work.
All authors are with The BioRobotics Institute, Scuola Superiore Sant'Anna, Pontedera (Pisa), Italy.

† Corresponding author: veronica.iacovacci@santannapisa.it
This work was supported by the European Commission under the Horizon Europe programme (REGO Project, Grant #101070066)

taken to design the carrier, Section III presents experimental settings and major results, and Section IV provides discussion and final conclusions on the work.

II. Materials and Methods

The proposed untethered carrier includes two operating units to support remotely controlled navigation and MMPs suspension release. Each unit was designed and dimensioned individually before studying the integration of the units and possible interferences.

A. Release Mechanism Design

Several strategies exist for delivering a liquid suspension. Among those, gas-based pressure generation in a liquid chamber [6, 17] and chamber squeezing mechanisms [18, 19] can be considered relevant examples.

Here, numerical analysis was performed to find the pressure needed to initiate MMPs suspension release either with a gradual (more than a minute) or one-shot (within several seconds) profile. COMSOL ® Multiphysics, Laminar Flow module was used for this purpose: a moving piston pushing the suspension out of a fluidic chamber was simulated to calculate the force needed to pump out all the fluid in the chamber.

A syringe-type mechanism was proposed in light of its simplicity and robustness. Simulation results allowed us to determine the necessary pushing force given the dimensions of internal components. The piston was actuated through permanent magnets by implementing a bistable mechanism based on two equilibrium configurations, here defined as loaded and released, respectively. A detailed view of the design is presented in Fig. 1a. The carrier includes 3 identical ring permanent magnets with axial magnetization. One of the magnets (m_2) is connected to the piston and is able to move, whereas the other two magnets (m_1 and m_3) are fixed. The piston does not move in the loaded configuration due to friction forces and calibration of the distance between the magnets inside the carrier: m_2 should be closer to m_1 in order to keep the piston fixed in the rest condition. Conversely, if m_2 is dragged towards m_3 by an externally applied magnetic field, the magnetic attraction force between m_2 and m_3 prevails, thus moving the piston to activate the release (released configuration).

The carrier can enter the released configuration only when being anchored in a fixed position (which can be achieved with the Fixing magnet M_F) and approached frontally by another external magnetic source (namely Release magnet M_R), which would move the m_2-piston system. Both configurations (loaded and released) are shown in Fig. 1b along with the employed external magnetic sources.

To allow the bistable mechanism to work, the distances between the three IPMs magnets should be properly set (Fig. 2). Inside the capsule, there are 3 main compartments: between the m_1 and m_2 (Δ_{12}), between the m_2 and m_3 (Δ_{23}), and the fluid chamber (Δ_{fluid}) between m_3 and the orifice. For consistency, m_3 is the magnet closest to the fluid chamber.

The variables in parentheses correspond to longitudinal distances. The carrier length is also affected by the magnets

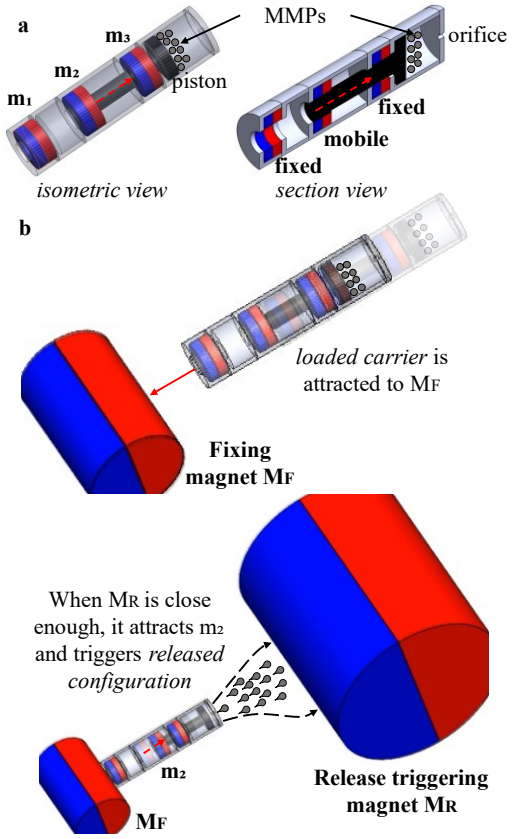

Figure 1. Novel Magnetic Carrier for MMPs suspension delivery: (a) carrier concept overview and components;(b) carrier in the loaded and released configurations.

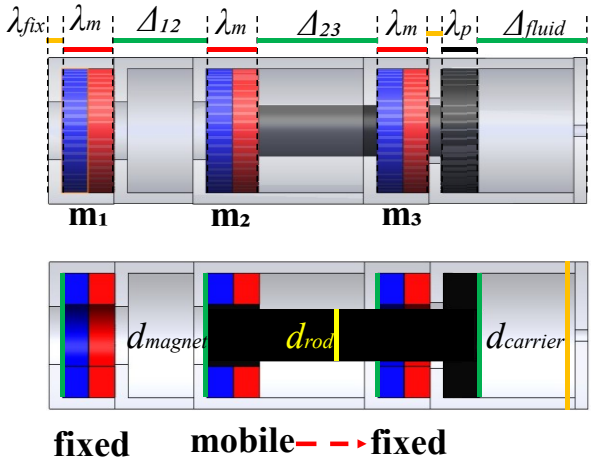

Figure 2. Carrier design specifications and dimensioning.

heights λ_m, by the thickness of the piston λ_p and of the magnets fixers λ_{fix}. All magnets were assumed to be identical. Therefore, the magnetic attraction force only varies with the distance between them. Consequently, $\Delta_{12} \leq \Delta_{23}$ is needed to guarantee m_2 and piston being locked in the loaded configuration. Additionally, Δ_{23} corresponds to the potential piston displacement during actuation, which can be seen in Fig. 2. Therefore, $\Delta_{23} = \Delta_{fluid}$ ensures efficient space use with piston stroke corresponding to the reservoir length. If we

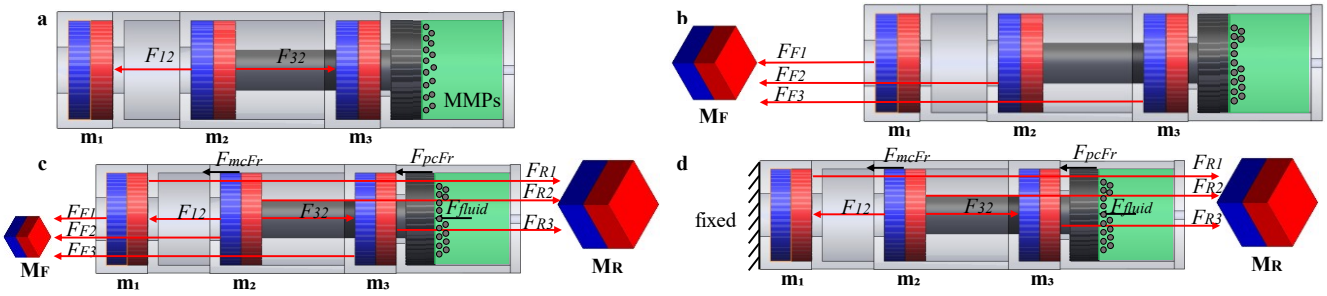

Figure 3. Force balance analysis in different configurations of the carrier and in the presence of external permanent magnets: (a) loaded configuration at rest, (b) navigation towards M_F, (c) release triggering of a magnetically fixed carrier, and (d) release triggering of a non-magnetically fixed carrier.

assume $\Delta_{12} = \Delta_{23} = \Delta_{fluid} = \Delta$, then the total carrier length can be calculated as:

$$Length = 3\lambda_m + 3\Delta + 2\lambda_{fix} + \lambda_p \quad (1)$$

The diameter is affected by carrier thickness and magnet diameter, i.e., $d_{carrier} = thickness + d_{magnet}$.

B. External permanent magnets dimensioning

An analytical model is aimed at understanding when the carrier is stable and how it interacts with the two external magnetic sources shown previously (F-fixing and R-releasing), which should be properly dimensioned to prevent interferences and guarantee correct operation. To this aim, the force diagrams acting on the carrier were drawn (Fig. 3) to derive the relevant equilibrium conditions.

The main variables in the analysis are magnet sizes and grades, the distance between IPMs, orifice size, fixing distance, and capsule material. Depending on available components, a number of realizations are possible: the prototype dimensions can be changed as long as we satisfy the conditions set below.

Magnetic forces between magnets (both external and internal) are approximated as dipole-dipole interaction and can be calculated with such assumptions as (2) when considering attraction between m_1 and m_2. Such approximation stands valid since magnets are at least $2\lambda_m$ times distant [20].

$$F_{12} = (3\, B_{r1}\, V_1\, B_{r2}\, V_2) / (2\, \mu_0 \pi\, r_{12}^4), \quad (2)$$

where B_r corresponds to the remanent magnetic flux density, V is the volume of the magnet, μ_0 is the vacuum permeability constant, and r is the distance between the dipoles.

Starting with a loaded configuration (Fig. 3a), it is important for m_2 and the connected piston to stay fixed in space. As mentioned, this can be achieved if the attraction force between m_1 and m_2 is higher than the one acting between m_2 and m_3:

$$F_{12} > F_{32} \quad (3)$$

Once we have a stable loaded carrier satisfying (3), it is important to navigate it towards the site of interest. An external driving magnet, either M_R or M_F, can be employed for this purpose. The external magnet attracts all carrier magnets and, hence, the carrier itself. The sum of these forces (F_{F1}, F_{F2}, and F_{F3}) (4) allows us to understand how much force can be exerted on the carrier to induce navigation. As the carrier would move towards the external magnet M_F, the latter should be placed close to the site of interest. Depending on the usage and local environment, relevant effects should be taken into account, such as gravity, buoyancy etc.

$$Locomotion\ Force = F_{F1} + F_{F2} + F_{F3} \quad (4)$$

Once a loaded carrier is at a target location, it should be magnetically anchored using M_F and then triggered to release the MMPs using M_R. This condition is illustrated in Fig. 3c-d along with relevant acting forces. F_{pcFr} and F_{mcFr} correspond to friction forces between the piston and carrier and between the magnet and carrier, respectively. $F_{R1\text{-}2\text{-}3}$ correspond to the magnetic attraction forces between internal magnets m_1, m_2, m_3 and the releasing external magnet M_R. Lastly, F_{fluid} indicates how much force a piston needs to generate in order to push the fluid, which is referenced from numerical simulation results. It is important to ensure the stability of the fixed loaded carrier: the force exerted by the releasing magnet should not be higher than the fixing force (5).

$$F_{F1} + F_{F2} + F_{F3} > F_{R1} + F_{R2} + F_{R3} \quad (5)$$

If the above equation is not satisfied, the carrier would simply detach and travel towards the releasing magnet.

At the same time, the magnetic field of the releasing magnet should be strong enough for the m_2, and hence the connected piston, to be attracted toward it and to push the suspension out (6).

$$F_{R2} + F_{32} > F_{F2} + F_{12} + F_{pcFr} + F_{mcFr} + F_{fluid} \quad (6)$$

Alternatively, if the capsule is anchored non-magnetically a single M_R would be sufficient to initiate the release:

$$F_{R2} + F_{32} > F_{12} + F_{pcFr} + F_{mcFr} + F_{fluid} \quad (7)$$

In each configuration, it is also crucial to find out if the released MMPs would escape the carrier magnetic field upon release. The magnetic attraction of the MMPs toward the releasing magnet ($F_{R\text{-}MMPs}$) should be greater than the cumulative action of fluid drag ($6r\pi\mu v_f$), the magnetic attraction of the MMPs toward the fixing magnet ($F_{F\text{-}MMPs}$), and the attraction of internal permanent magnets ($F_{IPMs\text{-}MMPs}$) to leave the carrier. Essentially, escaping velocity v_f can be derived from the following relation:

$$F_{R\text{-}MMPs} > 6\, r\, \pi\, \mu\, v_f + F_{IPMs\text{-}MMPs} + F_{F\text{-}MMPs} \quad (8)$$

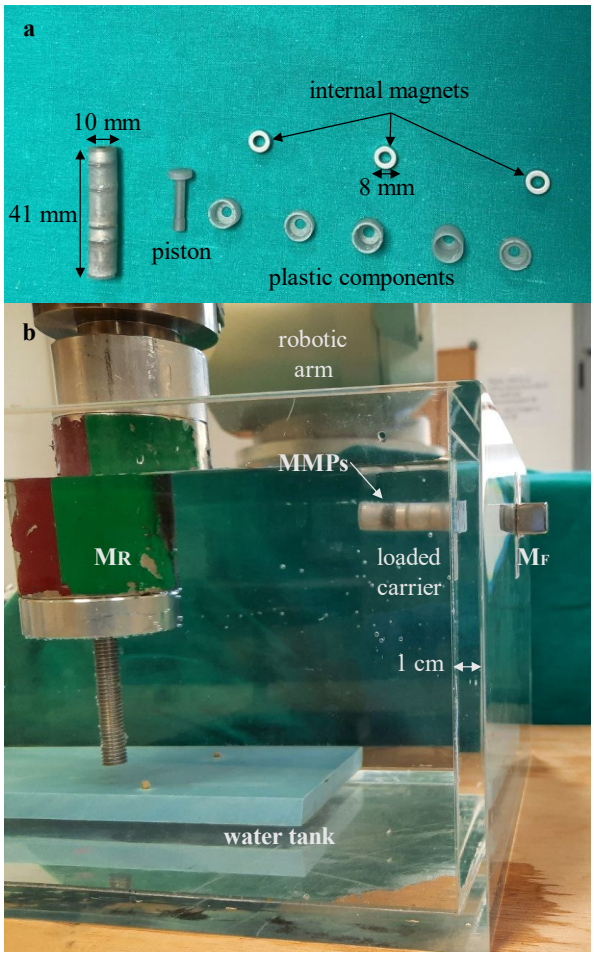

Figure 4. Experimental settings: (a) prototype and (b) testing set up.

III. Experiments and Results

By changing design parameters (IPM size, internal distances, EPMs sizes), analytical model revealed a number of possible carrier design realizations. Some trends were evident. First, the bigger the internal magnets are, the longer the capsule has to be in order to allow sufficient spacing between them: if IPMS are too close to each other, it is almost impossible to detach them with a counter-magnetic field (M_R). For example, if the overall carrier length has to be within 40 mm, each internal magnet has an upper bound of 8 mm in diameter. Second, friction forces play a major role when the carrier and its magnets become smaller: 3 mm in diameter magnets were found to be approximately a lower bound. Third, larger IPMs require the use of larger external magnets, both for fixing and releasing. Therefore, the capsule size is also governed by the external magnet sizes and operative workspace.

The next step was to frame the analytical results within certain practical conditions: available equipment and commercially available magnets. The biggest – yet manageable - available magnet was an N35 grade cylindrical magnet, 60 mm in diameter and 70 mm in height, which can work as either a releasing or fixing magnet. Iterations of available commercial magnet dimensions resulted in the choice of N35 grade ring IPMs that are 8 mm in diameter, 4 mm in height (λ_m), and with a 4.2 mm hole. Based on the above considerations, prototyping was made. The carrier components were fabricated using Form 3+ printer by Formlabs with a grey pro resin. A sample prototype and its components are displayed in Fig. 4a. Here, $\Delta = 8$ mm, $\lambda_p = 2$ mm, $d_{rod} = 4.2$ mm, and $\lambda_{fix} = 1$ mm. Fluid chamber accommodates 300 µl volume. Numerical simulations revealed F_{fluid} to be equal to 6.3 mN for this configuration.

Upon prototyping, both locomotion and MMPs suspension release were tested. An aqueous environment was chosen for a proof-of-concept validation as it is representative of major possible applications where a carrier could be manipulated, navigated, fixed, and triggered to release a MMPs suspension.

The testing platform (Fig. 4b) includes a water tank (10 x 10 x 30 cm) containing the carrier (41 x 10 mm), a fixing magnet (N52 5 mm cuboidal magnet), and a navigation/release-activation magnet (M_R - cylindrical magnet, 60 mm in diameter and 70 mm in height) mounted on a robotic arm (Melfa RV-3SB, Mitsubishi) allowing multiple degrees of freedom control.

A. Locomotion and MMPs Release Experiments

In this section, we validate the models and assess the systems in terms of locomotion, release of magnetic non-magnetic particle suspensions, and release of different particle suspension concentrations.

To prove locomotion capabilities, several common navigation modes were tested inside the water tank: magnetic dragging at air-water interface and underwater swimming (see the attached Video 1). A combination of navigation and fixing was also achieved both at air-water interface and under water (see Video 2). During navigation for target reaching, the external magnet M_F was placed more than 10 cm apart from the prototype, which coincides with analytical model predictions within a 0.5 cm error margin. The speed is around 14 mm/s or 0.33 body-length/s.

To switch from locomotion to release control, the release-triggering distance values were studied in order to validate the analytical model. In this approach, the robotic arm gradually moves M_R parallel to the carrier axis until the release mechanism is activated. At that point, the distance between M_R and the carrier was measured. A good accordance with the analytical model (5.8 mm predicted distance) was evident, as the minimal actuation distance was measured to be 6.4 ± 0.5 mm based on 20 repetitions.

The release was tested for magnetic and non-magnetic particles to demonstrate the suitability of the carrier to perform on-demand release of different types of cargo and to assess the suitability of the design (see Videos 3 and 4). Indeed, carrier design should prevent MMPs from sticking inside the internal carrier chamber due to magnetic attraction and the release behavior should be comparable for magnetic and non-magnetic cargoes.

5 µm NdFeB particles and 100 µm graphite particles were used in aqueous suspension as magnetic and non-magnetic cargoes, respectively. Fig. 5 shows the MMPs suspension release progression. NdFeB particles were ejected from the carrier and then attracted by M_R. On the other hand, non-

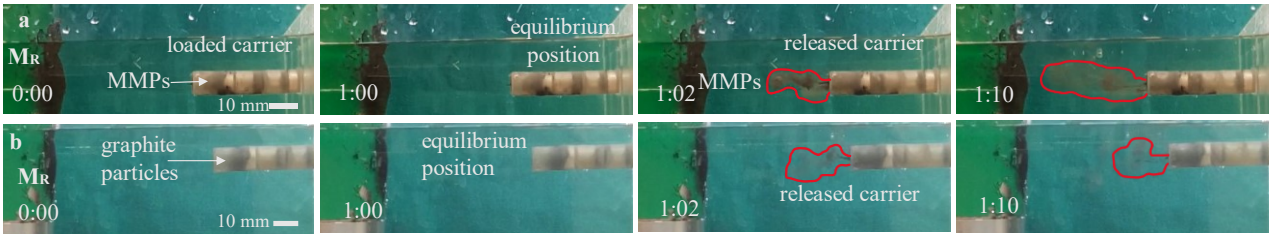

Figure 5. Progression of a magnetically fixed carriers release of (a) 5 µm NdFeB and (b) 100 µm graphite particles.

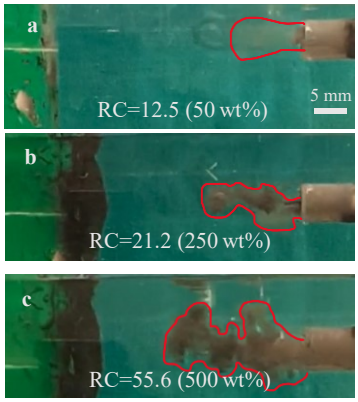

Figure 6. Release steps of a magnetically fixed carrier for different weight concentrations of NdFeB magnetic particles: (a) 50, (b) 250, and (c) 500 wt%.

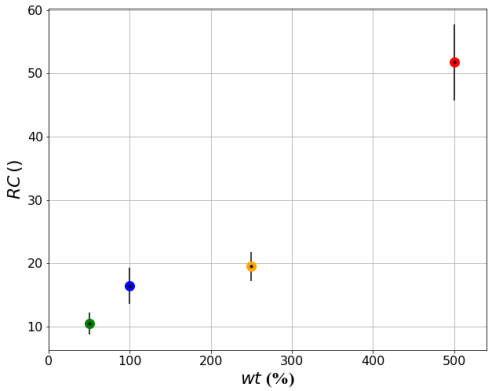

Figure 7. MMPs concentration and Release Coefficient correlation graph. Each point rapresents the Release Coefficient at a specific particles concetration.

magnetic graphite particles in Fig. 5b are shown to be floating once released.

Further analysis was performed to study the efficiency of the carrier in expelling its cargo, i.e., to find the percentage of released volume over the injected one. In the setting described above, the carrier was first filled with the suspension of MMPs or non-magnetic particles with the same concentration and then weighed. After the release task, the carrier was weighed again. It was then possible to find the difference in volume and thus the amount of released solution per release cycle. An average 25 ± 2% released MMPs suspension volume was calculated based on 20 repetitions. Regarding graphite particles, an average released volume was found to be 23 ± 2%, which means an approximately similar performance of the release actuation, i.e., magnetically controlled piston pushing.

In order to study the correlation between release efficiency and suspension features as well as to identify strategies to tune the number of particles released; particle suspension concentration was also varied over tests. For this purpose, the carrier was fully loaded, which corresponds to 300 µl reservoir, with a suspension of NdFeB particles in water with different MMPs weight concentrations (50, 100, 250, and 500 wt%). The percentage of released particles was evaluated through image analysis using the open-source software ImageJ by studying the number of gray pixels, which correspond to released particles, in an enclosed area. A custom metric was introduced, namely the release coefficient *RC*, which can be calculated as:

$$RC = (Area \cdot BGV)/(1000 \cdot MGV), \quad (9)$$

where *Area* is the total number of pixels in the enclosed area saturated with released MMPs, *MGV* is the mean gray value within this area, and *BGV* is the mean gray value of a background sample in an image to account for different lighting.

The darker the ejected MMPs cluster is on the image, the more saturated this region is (i.e., has more MMPs) which would correspond to a small value of MGV (0 – dark, 255 – white). Otherwise, if there are not many magnetic particles, the *MGV* value would be higher, i.e., the area would be brighter. Several release examples are given in Fig. 6. For each concentration, the frames of 10 release repetitions were analyzed to derive the mean RC value. In Fig. 7, the mean RC values and standard deviations are given for different weight concentrations. As evident in Fig. 7, the introduced metric *RC* correlates with the number of loaded particles and increases as the concentration increases. Furthermore, the results in the figure suggest a stable and repeatable release profile. Furthermore, no premature release was recorded during the release experiments.

IV. Discussions and Conclusion

The proposed magnetic carrier proved able to perform controlled target reaching due to remote magnetic control and on-demand cargo release of both non-magnetic and magnetic cargoes with different concentrations. The model-derived design confirmed simulations and analytical predictions with relatively low errors taking into account several assumptions made during design. This gives us the opportunity to devise size modifications in the carrier to better fit potential application scenarios and to derive design series (internal and

external magnet sizes, carrier component dimensions) by leveraging model predictions.

The carrier design proved to be efficient in releasing MMPs even in high concentration suspensions despite the presence of IPMs. Besides, the internal magnets presumably helped to keep the particles inside the reservoir and to avoid premature release, which is crucial for biomedical applications. Nevertheless, the released MMPs were shown to escape the magnetic field of the capsule, being available for further remote actuation using external magnets (e.g. for hyperthermia activation or deeper target reaching).

However, a relatively small release volume was recorded. One of the major reasons for such performance is prototype imperfections and consequent bad sealing of the MMPs suspension chamber. As the piston is likely to not fully fit the inner walls, some liquid may travel from the suspension chamber toward internal magnets. However, the same behavior was evident in the cases of both non-magnetic and magnetic suspension releases. Therefore, the use of magnetic particles does not change the performance of the proposed carrier. At the same time, tight-fitting or interference is undesired since the friction forces would rise dramatically. Some modifications of the piston or suspension chamber are thus needed to guarantee a higher suspension release volume.

A strong asset of the proposed carrier is its repeatability. All the experiments were repeated consistently 20 times revealing low variability (<5%). Furthermore, a straightforward re-loading could be performed: a released carrier simply needs to be approached from the rear with a strong attracting magnet, which would move the m_2 and, hence, the piston from an unloaded position back to the loaded position. This opens up other possible venues and gives the opportunity to use the carrier for sampling as well.

To further mitigate the risk of premature release, flexible membrane or size modifications of the outlet orifice can be foreseen in the future.

The proposed system stands as extremely flexible in terms of actuation. Indeed, as demonstrated in Video 2, appropriate dimensioning and distancing of fixing and releasing magnets can result in locomotion and on-demand release in several relevant scenarios.

Overall, in this work we proposed a versatile untethered carrier with on-demand MMPs suspension release capabilities and, hence, high targeting efficiency. To design it, numerical simulations and analytical studies were implemented. A parametrization was followed at each step with corresponding variables indicated. The results demonstrate a fully functional untethered system which is a novelty in the MMPs delivery research.

V. References

[1] P. M. Martins, A. C. Lima, S. Ribeiro, S. Lanceros-Mendez and P. Martins, "Magnetic nanoparticles for biomedical applications: From the soul of the Earth to the deep history of ourselves," *ACS Applied Bio Materials,* vol. 4, no. 8, pp. 5839-5870, 2021.

[2] A. E. Kabeel, E. M. El-Said and S. A. Dafea, "A review of magnetic field effects on flow and heat transfer in liquids: Present status and future potential for studies and applications.," *Renewable and Sustainable Energy Reviews,* vol. 45, pp. 830-837, 2015.

[3] P. M. Price, W. E. Mahmoud, A. A. Al-Ghamdi and L. M. Bronstein, "Magnetic Drug Delivery: Where the Field Is Going," *Frontiers in Chemistry,* vol. 6, 2018.

[4] L. Ricotti, A. Cafarelli, V. Iacovacci, L. Vannozzi and A. Menciassi, "Advanced micro-nano-bio systems for future targeted therapies," *Current Nanoscience,* vol. 11, no. 2, pp. 144-160, 2015.

[5] S. Wilhelm, A. J. Tavares, Q. Dai, S. Ohta, J. Audet, H. Dvorak and W. C. Chan, "Analysis of nanoparticle delivery to tumours," *Nature reviews materials,* vol. 1, no. 5, pp. 1-12, 2016.

[6] K. T. Nguyen, M. C. Hoang, E. Choi, B. Kang, J.-O. Park and C.-S. Kim, "Medical microrobot — a drug delivery capsule endoscope with active locomotion and drug release mechanism: Proof of concept," *International Journal of Control, Automation and Systems,* vol. 18, no. 1, pp. 65-75, 2019.

[7] S. M. Mirvakili and R. Langer, "Wireless on-demand drug delivery," *Nature Electronics,* vol. 4, pp. 464-477, 2021.

[8] F. Munoz, G. Alici and W. Li, "A magnetically actuated drug delivery system for robotic endoscopic capsules," *Journal of Medical Devices,* vol. 10, no. 1, 2015.

[9] J. Sikorski, C. M. Heunis, R. Obeid, V. K. Venkiteswaran and S. Misra, "A flexible catheter system for ultrasound-guided magnetic projectile delivery," *IEEE Transactions on Robotics,* vol. 38, no. 3, pp. 1959-1972, 2022.

[10] N. Li, C. Tous, I. P. Dimov, D. Cadoret, P. Fei, Y. Majedi, S. Lessard, Z. Nosrati, K. Saatchi, U. O. Hafeli, A. Tang, S. Kadoury, S. Martel and G. Soulez, "Quantification and 3D localization of magnetically navigated superparamagnetic particles using MRI in Phantom and swine Chemoembolization Models," *IEEE Transactions on Biomedical Engineering,* vol. 69, no. 8, pp. 2616-2627, 2022.

[11] M. C. Hoang, V. H. Le, J. Kim, E. Choi, B. Kang, J.-O. Park and C.-S. Kim, "Untethered robotic motion and rotating blade mechanism for actively locomotive biopsy capsule endoscope," *IEEE Access,* vol. 7, pp. 93364-93374, 2019.

[12] D. Ye, J. Xue, S. Yuan, F. Zhang, S. Song, J. Wang and M. Q.-H. Meng, "Design and control of a magnetically-actuated capsule robot with biopsy function," *IEEE Transactions on Biomedical Engineering,* vol. 69, no. 9, pp. 2905-2915, 2022.

[13] S. Yim, K. Goyal and M. Sitti, "Magnetically actuated soft capsule with the multimodal drug release function," *IEEE/ASME Transactions on Mechatronics,* vol. 18, no. 4, pp. 1413-1418, 2013.

[14] V. H. Le, H. L. Rodriguez, C. Lee, G. Go, J. Zhen, V. D. Nguyen, H. Choi, S. Y. Ko, J.-O. Park and S. Park, "A soft-magnet-based drug-delivery module for active locomotive intestinal capsule endoscopy using an electromagnetic actuation system," *Sensors and Actuators A: Physical,* vol. 243, pp. 81-89, 2016.

[15] G. Ciuti, P. Valdastri, A. Menciassi and P. Dario, "Robotic magnetic steering and locomotion of capsule endoscope for diagnostic and surgical endoluminal procedures," *Robotica,* vol. 28, no. 2, pp. 199-207, 2009.

[16] G. Ciuti, R. Donlin, P. Valdastri, A. Arezzo, A. Menciassi, M. Morino and P. Dario, "Robotic versus manual control in magnetic steering of an endoscopic capsule," *Endoscopy,* vol. 42, no. 2, pp. 148-152, 2009.

[17] S. Guo, Y. Hu, J. Guo and Q. Fu, "Design of a novel drug-delivery capsule robot," in *IEEE International Conference on Mechatronics and Automation (ICMA)*, 2021.

[18] I. Wilding, P. Hirst and A. Connor, "Development of a new engineering-based capsule for human drug absorption studies," *Pharmaceutical Science & Technology Today,* vol. 3, no. 11, pp. 385-392, 2000.

[19] D. Son, H. Gilbert and M. Sitti, "Magnetically actuated soft capsule endoscope for fineneedle biopsy," *Soft Robotics,* vol. 7, no. 1, pp. 10-21, 2020.

[20] A. J. Petruska and J. J. Abbott, "Optimal Permanent-Magnet Geometries for Dipole Field Approximation," *IEEE Transactions on Magnetics,* vol. 49, no. 2, pp. 811-819, 2013.